



- 1 Ocean acidification alters phytoplankton diversity and community structure in the coastal
- 2 water of the East China Sea
- 3 Yuming Rao^{#1}, Na Wang^{#2}, He Li³, Jiazhen Sun², Xiaowen Jiang², Di Zhang², Liming Qu², Qianqian
- 4 Fu², Xuyang Wang², Cong Zhou², Zichao Deng², Yang Tian², Xiangqi Yi², Ruiping Huang², Guang
- 5 Gao², Xin Lin² and Kunshan Gao^{*1, 3}
- 6 State Key Laboratory of Marine Environmental Science, College of the Environment and Ecology,
- 7 Xiamen University, Xiamen, China
- 8 ² State Key Laboratory of Marine Environmental Science, College of Ocean and Earth Science,
- 9 Xiamen University, Xiamen, China
- 10 ³ Co-Innovation Center of Jiangsu Marine Bio-industry Technology, Jiangsu Ocean University,
- 11 Lianyungang 222005, China
- 12 # These authors contributed equally to this work
- * Correspondence: ksgao@xmu.edu.cn
- 14 Keywords: CO₂, East China Sea, mesocosms; ocean acidification; phytoplankton; primary
- 15 production
- 16 Abstract
- Anthropogenic CO₂ emissions and their continuous dissolution into seawater lead to seawater
- 18 pCO₂ rise and ocean acidification (OA). Phytoplankton groups are known to be differentially
- 19 affected by carbonate chemistry changes associated with OA in different regions of contrasting
- 20 physical and chemical features. To explore responses of phytoplankton to OA in the Chinese coastal
- 21 waters, we conducted a mesocosm experiment in a eutrophic bay of the southern East China Sea
- 22 under ambient (410 μatm, AC) and elevated (1000 μatm, HC) pCO₂ levels. The HC stimulated
- 23 phytoplankton growth and primary production during the initial nutrient-replete stage, while the
- 24 community diversity and evenness were reduced during this stage due to the rapid nutrient
- 25 consumption and diatom blooms, and the subsequent shift from diatoms to hetero-dinoflagellates
- 26 led to a decline in primary production during the mid and later phases under nutrient depletion. Such
- 27 suppression of diatom-to-dinoflagellate succession occurred with enhanced remineralization of
- 28 organic matter under the HC conditions, with smaller phytoplankton becoming dominant for the
- 29 sustained primary production. Our findings indicate that, the impacts of OA on phytoplankton





diversity in the coastal water of the southern East China Sea depend on availability of nutrients, with primary productivity and biodiversity of phytoplankton reduced in the eutrophicated coastal water.

1 Introduction

It is commonly known that sequestration of CO_2 in coastal waters play important roles against global warming due to their high primary productivity (Rogelj et al., 2022), which resulted in faster CO_2 removal due to photosynthesis than dissolution of CO_2 from the air (Stukel et al., 2023). It has been assessed that, with the increasing anthropogenic CO_2 emissions, the oceanic CO_2 sink increased from 1.7 ± 0.4 pg C yr⁻¹ in the 1980s to 2.5 ± 0.6 pg C yr⁻¹ in the 2010s (Friedlingstein et al., 2025). Nevertheless, such apparent oceanic CO_2 uptake is altering carbonate chemistry in surface oceans, leading to a pH drop of by 0.017-0.027 units per decade, with a potential further drop by 0.3-0.4 units at the end of this century (Canadell et al., 2023; Gattuso et al., 2015). Such progressive ocean acidification (OA) has been shown to impact many marine organisms (Gattuso et al., 2015), including primary producers (Gao et al., 2020), subsequently feeding back on the CO_2 sequestration efficiency in marine systems including coastal waters.

OA in eutrophic coastal waters are suggested to progress faster than in open oceans by roughly 20 % due to CO_2 dissolution and enhanced remineralization of organic maters (Cai et al., 2011). The subsequent changes in carbonate chemistry may thus drive shifts in phytoplankton community structures/diversity and affect primary productions in differential ways due to regional environmental traits and species-specific physiology (Feng et al., 2024; Gao et al., 2012). While the effects of elevated pCO_2 on different phytoplankton assemblages have been demonstrated, positive, neutral and negative effects have been reported, reflecting differences in experimental approaches and/or phytoplankton compositions (Gao et al., 2020). Among the different approaches, field mesocosm experiments under elevated pCO_2 projected for future OA scenario have been employed to investigate the effects of OA on ecological processes, including primary production. Previous mesocosm experiments showed reduced growth of coccolithophores species under 710 μ atm pCO_2 during early summer in 2001 (Engel et al., 2005) and the loss of the ability to form blooms under 1000–3000 μ atm pCO_2 during early summer in 2011 (Riebesell et al., 2017). Under elevated pCO_2 , the phytoplankton communities in Norwegian coastal mesocosms shifted from Bathycoccus to

60

6162

63

64

65

66 67

68 69

70

71

72

73

7475

76

7778

79

80

81

82

83

84

85 86

87





Micromonas (Meakin and Wyman, 2011). By contrast, another mesocosm experiment carried out in northeast Atlantic showing that diatoms were insensitive to OA under oligotrophic conditions, but were positively affected under nutrient enrichment (Bach et al., 2019). Previously, we showed, by running a mesocosm experiment during spring of 2018 in the southern coastal water of the East China Sea, that elevated pCO₂ of 1000 µatm suppressed the succession from diatoms to dinoflagellates and increased the abundance of viruses and heterotrophic bacteria, thereby promoting refueling of nutrients for phytoplankton growth (Huang et al., 2021). These results indicate that the effects of OA on community structure can vary temporally and spatially. On the other hand, mesocosm experiments conducted in oligotrophic or mesotrophic regions showed that nutrients enrichment increased Chl a concentration under high pCO₂ condition (Riebesell et al., 2017; Tanaka et al., 2013; Schulz et al., 2013), however, mesocosm experiments conducted in highly eutrophic water showed that high pCO₂ did not affect Chl a concentration (Liu et al., 2017; Huang et al., 2021). Plankton communities supported by remineralized nutrients were more sensitive to OA than those having access to higher availability of inorganic nutrients (Bach et al., 2016; Bach et al., 2019). It is likely that availabilities or levels of eutrophication can modulate the effects of OA, alongside regional chemical and physical differences (Paul and Bach, 2020). In coastal regions, changes in seawater carbonate chemistry influence primary production which in reverse affect the pH change due to faster photosynthetic CO₂ removal than its dissolution (Gao, 2021), resulting in increased pH during daytime and declined pH during nighttime. Such large diel pH fluctuation may require phytoplankton to invest more energy to maintain cellular homeostasis in response to the negative effects of increased hydrogen ion concentration (the acidic stress), thereby affecting the functioning of planktonic ecosystem (Raven and Beardall, 2020; Rokitta et al., 2012; Taylor et al., 2017). The documented positive effects of increased inorganic carbon substrates (e.g., CO₂ and HCO₃⁻) and the negative effect of increased H⁺ concentration may shape the responses of coastal ecosystems to OA, leading to controversial results (Wu et al., 2017; Vázquez et al., 2023; Chauhan et al., 2024). To better understand the consequences of OA in Chinese eutrophic coastal regions, we conducted a mesocosm experiment in the eutrophic coastal water of Wuyuan Bay, Xiamen, China, using in situ plankton communities during October-December, 2019 and investigated how OA shapes the diversity of phytoplankton community and affects primary

93

94

95

96

97

98

99

100101

102

103

104

105

106

107

108

109

110

111

112113

114115

116





production processes. Our results show that in the eutrophic coastal water of East China Sea, with the natural decrease of temperature, elevated *p*CO₂ increased primary production by promoting the

phytoplankton biomass (indicated by Chl a concentration) under nutrient-replete condition, and

91 promoted smaller phytoplankton's growth to sustain the primary production after the nutrient

92 depletion and diatom bloom collapsed, though suppressed the emergence of dinoflagellates.

2 Materials and methods

2.1 Mesocosms setup and sampling

The in situ mesocosm experiment was conducted at the Facility for the Study of Ocean Acidification Impacts of Xiamen University (FOANIC-XMU) located in the subtropical coastal region Wuyuan Bay of southern East China Sea (24.52°N, 117.18°E) from 9th October (day 0 relative to algal inoculation) to 14th November, 2019. Nine cylindrical and transparent thermoplastic polyurethane (TPU) mesocosm bags, each 3 m deep and 1.5 m in diameter, were filled with approximately 3000 L of in situ seawater that had been prefiltered (MU801-4T, Midea, China, pore size of 0.01 μm). The mesocosms were hooked to and secured within steel frames. Two pCO₂ treatments were established to investigate the effects of ocean acidification on the in situ phytoplankton community: an ambient pCO₂ treatment (AC, 410 μatm; 4 numbered bags) and a high pCO₂ treatment representative of end-of-century projections (HC, 1,000 µatm; 5 numbered bags). To adjust CO₂ in seawater in the HC bags to the projected 1000 µatm in 2100s, approximately 11 L of CO₂-saturated seawater was added to each HC bag. The AC and HC pCO₂ levels were maintained by bubbling with ambient air and pre-mixed air-CO₂ (1000 µatm CO₂), respectively, at a rate of 5 L min⁻¹ using a CO₂ Enricher (CE-100B, Wuhan Ruihua Instrument & Equipment Ltd, China). After the carbonate system had been stabilized (leveled pH), 720 L of in situ seawater were filtered by a 180 µm mash to exclude large zooplankton, and each mesocosm bag was inoculated with 80 L of it to initiate the coastal microbial community. Samples were taken from each bag at a depth of 0.5m at 9:00 a.m. by niskin bottles every 1-3 days for physical, chemical and biological analysis.

2.2 Measurement of environmental factors

Solar light intensity was monitored every minute throughout the experimental period using a real-time solar irradiance monitoring device (EKO, Japan). Salinity, temperature and pH in each





117 mesocosm were measured with a salinometer, a digital thermometer and a pH meter (Orino 2 STAR, Thermo Scientific, U. S. A, calibrated with standard NBS buffer), respectively. Dissolved inorganic 118 119 carbon (DIC) was sampled and measured using an Environmental Water Analyzer (Ma et al., 2018), 120 and total alkalinity (TA) measured using an Automated Spectrophotometric Analyzer (Li et al., 121 2013). Other seawater carbonate chemistry parameters were calculated with CO2SYS software with 122 known parameters of pCO₂, salinity, pH, temperature, and nutrient concentration. 123 Nutrient samples of each bag were filtered through 0.45 mm cellulose acetate membrane, and the filtrate was divided into 2 subsamples; one was stored at -20 °C for the measurement of 124 125 NO₃⁻+NO₂⁻, PO₄³⁻, and NH₄⁺; another stored at 4°C for the measurement of SiO₃²⁻. Measurement of NO₃⁻+NO₂⁻, PO₄³⁻, and SiO₃²⁻ concentration was conducted using an auto-analyzer (AA3, Seal, 126 127 Germany), NH₄⁺ was measured with indophenol blue spectrophotometry using a spectrophotometer 128 (Tri-223, Spectrum, China) at 25 °C. 129 2.3 Measurement of chlorophyll a and particle organic matters 130 Water samples of each mesocosm (100 - 1000 mL, depending on the biomass in the 131 mesocosms) were filtered onto GF/F filter (Whatman, United States) by suction filter with low 132 vacuum pressure no more than 0.02 MPa and soaked in 5 mL pure methanol overnight. The extracts 133 were centrifuged at 8000 × g and 4 °C for 10 min, then the absorption spectra of supernatants from 134 400 to 800 nm were measured using a UV-VIS spectrophotometer (DU 800, Beckman, U. S. A). 135 The Chl a concentration was calculated according to the following equation (Ritchie, 2006): 136 Chl $a (\mu g L^{-1}) = 16.29 \times (A665 - A750) - 8.54 \times (A652 - A750)$ 137 where A750, A665, and A652 represents the absorbance of Chl a at wave length 750, 665, and 138 652 nm, respectively. 139 For the analysis of particulate organic carbon (POC) and nitrogen (PON) across two particle 140 size fractions, water samples of known volume were first filtered through a 20 µm mash to obtain 141 subsamples containing particle organic matters smaller than 20 µm. Particles larger than 20 µm 142 (retained on 20 µm mesh) were backwashed using an equal volume of prefiltered (0.22 µm) in situ seawater, yielding in subsamples containing particulate organic matters larger than 20 µm. All 143 subsamples were then filtered on pre-combusted (450 °C, 6 h) GF/F filter (Whatman) and stored at 144 -20 °C until analysis. Before analyses, all filters were fumed over pure HCl for 12 h and dried at 145





Before sunrise, 120 mL of water samples from each mesocosm were collected and dispensed into six 25 mL borosilicate bottles (three bottles for 12 h incubations, and three for 24 h incubations). For each culture duration of each mesocosm, two bottles were illuminated under natural light and one bottle was wrapped tightly in aluminum foil as a dark control. After incubation, cells were filtered onto the GF/F filters (Whatman) under dim light and stored at –20 °C. Before measurement, filters were placed individually in 20 mL scintillation vials and exposed to HCl fumes overnight, dried in a constant temperature oven at 60 °C for over 6 h to remove any unincorporated H¹⁴CO₃⁻. The incorporated ¹⁴C by algae was counted with a liquid scintillation counter (Beckman, LS6500, Germany) in the presence of 5 mL scintillation cocktail (Hisafe 3, Perkin-Elmer, United States). Nighttime respiratory carbon loss was calculated as the difference between carbon fixation over 12 h (daytime primary productivity) and 24 h (daily net primary productivity).

2.5 Determination of phytoplankton biomass and community structure

Water samples (500–2000 mL) from each mesocosm were collected into polyethylene bottles

and fixed with 1.5 % lugol's iodine. The samples were statically placed and concentrated into 50

mL subsamples in the centrifuge tube using siphons within 3 days. The concentrated subsamples

were examined with a microscopy (Nikon Eclipse Ns2) and a plankton counting chamber to assess

phytoplankton abundance and diversity based on the morphological characteristics as previous

described (Hasle and Syvertsen, 1997; Steidinger and Jangen, 1997; Yang and Liu, 2018). To

distinguish whether dinoflagellates are autotrophic or heterotrophic, we observed living algal cells

in the unstained water samples under the microscope for cell transparency and the presence of

60 °C to remove inorganic carbon, then packed in tin cups and measured with a CHNS elemental

analyzer (Vario EL cube Elementar, Germany).

2.4 Net primary production and dark respiration

chloroplasts, as shown in Fig. S9. For cell counts, an aliquot of $100~\mu L$ for each mesocosm was loaded onto a counting chamber for microscopic enumeration. In each aliquot, the count was deemed valid only when the total number of cells exceeded 200; otherwise, the subsample volume for microscopy was increased to achieve sufficient counts. For samples collected during the exponential growth phase that exhibited excessively high cell densities, appropriate dilution with $0.22~\mu m$ –filtered, sterilized seawater was





performed prior to counting (State Oceanic Administration 2005).

2.6 Statistical analysis

176

177178

179

180

181

182

183

184185

186

The data were all expressed by the mean and standard deviation (means \pm SD) and plotted by Origin 2024. Independent-samples *t*-test was conducted to check the significant effects of increased $p\text{CO}_2$ at the level of p < 0.05 using SPSS 19. To evaluate α -diversity, Shannon diversity index was calculated based on the relative abundances of phytoplankton taxa using the estimate R and diversity functions from the vegan package (version 2.6-4) in R (Version 4.2.2). Shannon index incorporates both species diversity and evenness. Patterns of physiological parameters over time were emphasizing using generalized additive models (GAMs) and constructed using the 'mgcv' package in R to analyze changes in physiology through the experiment.

3 Results

3.1 Environmental changes in the mesocosms

Throughout the experiment, most days were sunny, with daytime mean PAR (12h-average 187 188 photosynthetic active radiation) ranging from 200 to 850 µmol photons m⁻² s⁻¹ (Fig. S1). The environmental temperatures decreased gradually from 26.7 ± 0.05 °C at day 0 (9th October) to 21.1 189 190 \pm 0.28 °C at day 38 (14th November) (Fig. 1 a). Significant differences in pH_{NBS} and pCO₂ between 191 HC and AC were maintained throughout most of the experimental period, while there's no 192 significant difference in total alkalinity (TA) between the two pCO₂ treatments ($p = 4.02 \times 10^{-8}$, 2.87×10^{-12} , 0.549, respectively. Figs. 1 b-d, S5 a-c). 193 194 Following a sharp increase in phytoplankton biomass from Day 4 to Day 8 (Fig. 3 a), the pH_{NBS} 195 in the HC and AC mesocosms increased and peaked at 8.24 ± 0.16 and 8.56 ± 0.14 , respectively (Fig. 1 b). Correspondingly, the pCO_2 value dropped to the lowest points of 238.48 \pm 49.02 μ atm 196 197 (HC) and $82.82 \pm 32.88 \,\mu atm$ (AC) (Fig. 1 c). Then, as the phytoplankton biomass decreased after 198 day 8, pH_{NBS} gradually declined and pCO₂ increased, both stabilizing at relatively constant levels from day 18 until the end of experiment. There were no obvious temporal changes observed in total 199 200 alkalinity (TA) throughout the experiment (Fig. 1 d).



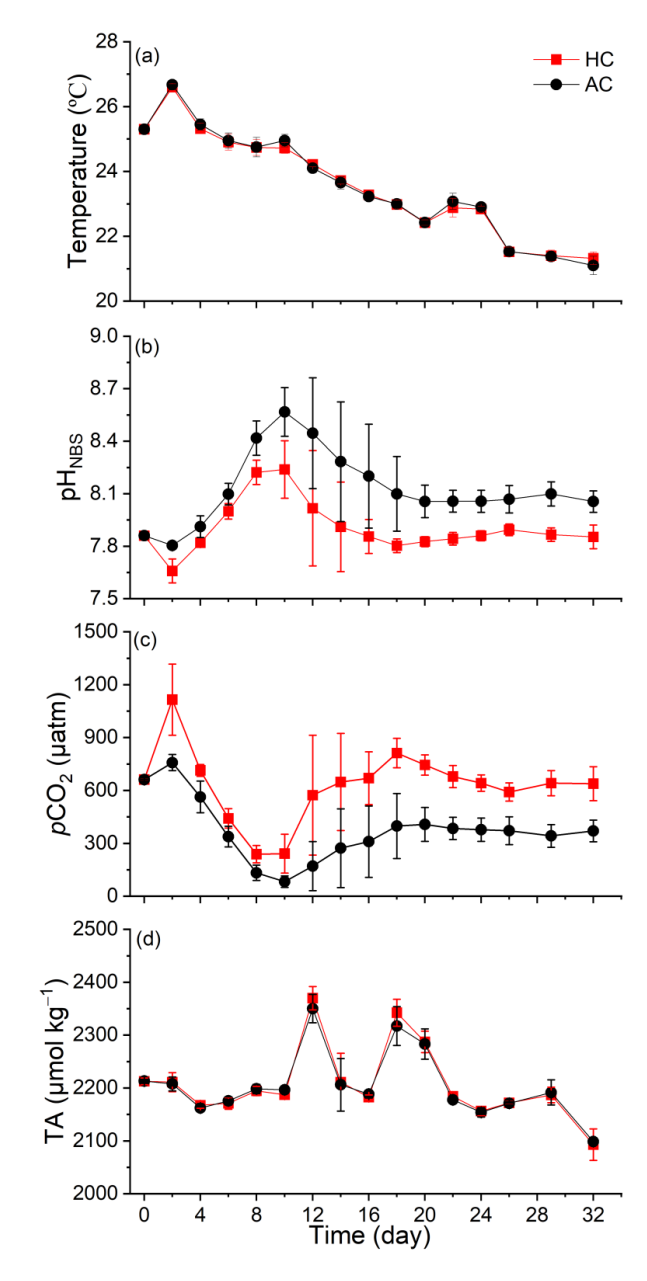


Figure 1. Temporal variation of seawater temperature (a), pH_{NBS} (b), pCO_2 (c) and TA (d) in HC (1000 μ atm) and AC (410 μ atm) mesocosms. The pCO_2 was estimated from the measured pH_{NBS} and DIC concentration using the CO2SYS program. Data are means \pm SD of 5 replicates for HC and 4 replicates for AC mesocosms.

201202

203

204



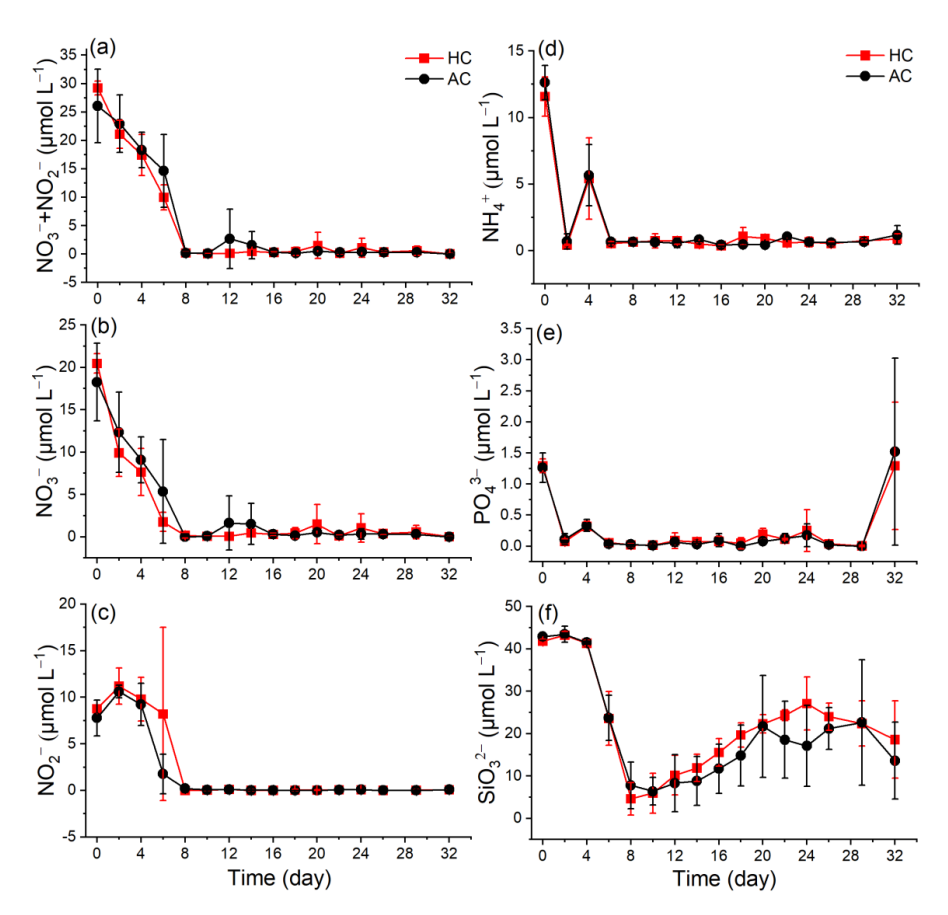


Figure 2. Temporal variation of nutrients (NO₃⁻, NO₂⁻, NO₃⁻+NO₂⁻, NH₄⁺, PO₄³⁻, and SiO₃²⁻) in HC (1000 μ atm) and AC (410 μ atm) mesocosms. Data are means \pm SD of 5 replicates for HC and 4 replicates for AC mesocosms.

The initial nutrient concentrations reflected the eutrophic condition in the coastal seawater (NO₃⁻+NO₂⁻: 27 μM, PO₄³⁻: 1.4 μM). In the mesocosm bags, nutrient concentrations declined dramatically in the early phase (up to day 8, Fig. 2). The NO₃⁻+NO₂⁻ and NO₃⁻ concentrations decreased sharply to nearly 0 by day 8 (Fig. 2 a, b). In contrast, the NO₂⁻ concentration experienced a slight increase on day 2, then declined to nearly 0 by day 8 and remained at a low level until the end of experiment in both HC and AC mesocosms (Fig. 2 c). Under HC condition, the NO₃⁻ concentration decreased more rapidly than that under the AC until day 20, although the difference





was not significant (p=0.423, Fig. S5 d). Both NH₄⁺ and PO₄³⁻ concentrations dropped to nearly 0 after 4 days and remain relatively stable thereafter. There were no significant difference observed between HC and AC mesocosms (p=0.579 and 0.631, respectively, Figs. 2 d, e, S5 e, f). The SiO₃²⁻ concentration decreased from $41.81 \pm 0.48 \,\mu\text{M}$ in HC and $42.88 \pm 0.91 \,\mu\text{M}$ in AC on day 0 to a minimum of $4.62 \pm 3.82 \,\mu\text{M}$ and $7.79 \pm 5.52 \,\mu\text{M}$ by day 8, respectively. Thereafter, SiO₃²⁻ concentrations in both HC and AC mesocosms gradually increased until the end of experiment (p=0.343, Figs. 2 f, S5 g).

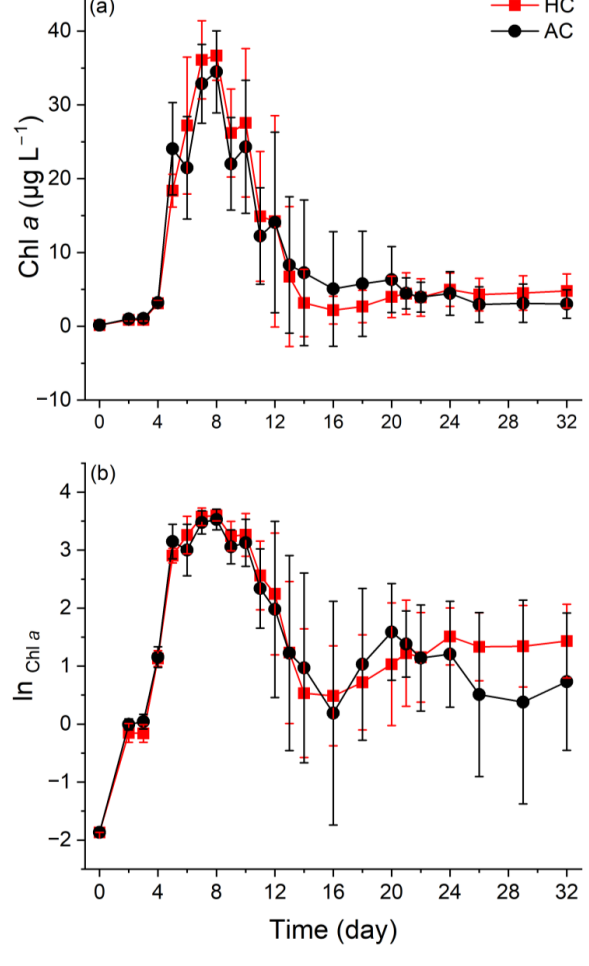


Figure 3. Temporal variations of Chl a concentration (a) and the LN scale of Chl a concentration (b) in HC (1000 μ atm) and AC (410 μ atm) mesocosms. Data are means \pm SD of 5 replicates for HC and 4 replicates for AC mesocosms.





3.2 Chlorophyll a concentration

Phytoplankton biomass, indirectly indicated by Chl a concentration, increased to peak at 35.88 \pm 3.25 µg L⁻¹ in the HC and 36.54 \pm 4.88 in the AC mesocosms on day 8, and then gradually decreased to 1.12 ± 0.43 µg L⁻¹ in HC by day 14 and 0.58 ± 0.31 µg L⁻¹ in AC by day 16, followed by a slight increase by the end of experiment (Fig. 3 a). Based on the natural logarithm (ln) scale of Chl a concentration, the phytoplankton growth kinetics under the two pCO $_2$ treatments showed the following phases (Fig. 3 b): the exponential phase (from day 0 to day 5), the stationary phase (from day 6 to day 10), the decline phase (from day 11 to day 16), and a second exponential phase from day 17 to day 24 in the HC and to day 20 in the AC mesocosms. Then, phytoplankton assemblages in the HC mesocosms entered a second stationary phase until the end of experiment, while in the AC ones, they entered a decline phase until day 29, followed by a slight increase on day 32.

Throughout the experiment, the elevated pCO $_2$ resulted in higher average value of Chl a concentration at most sampling times, although the differences were not statistically significant (p

3.3 Primary production and dark respiration

= 0.142, Fig. S5 h).

The primary production and night-respiratory per water volume showed patterns similar to those of phytoplankton biomass (indicated by Chl a concentration) (Fig. 4, a, b and c). They reached their maximal values on day 6, which corresponded to the end of exponential phase. As the phytoplankton communities entered the stationary phase, daytime (12 h) primary production, daily (24 h) net primary production and nighttime respiration per water volume progressively decreased, and then slightly increased again when the phytoplankton communities underwent the second exponential phase. The elevated pCO_2 increased both daytime and daily net primary production during the middle phase of the experiment, although the positive effect on 24 h primary production tended to decline by the end of experiment (p = 0.038 and 0.012, Fig. S6 a, b). The nighttime respiration of phytoplankton was suppressed before day 8 and enhanced thereafter under the elevated pCO_2 , though no significant difference was observed (p = 0.444, Fig. S6 c).

Primary productivity per Chl *a* increased sharply on day 4, and decreased to the lowest values on day 8. On day 12, both daytime and 24 h primary productivity in the HC increased drastically and then remained relatively stable until the end of experiment (Fig. 4 d, e). In contrast, two





additional peaks were observed in the AC mosocosms on days 16 and 26. The elevated pCO_2 appeared to have enhanced primary productivity from day 2 to day 20, though these effects were not statistically significant (p = 0.946 for daytime and p = 0.985 for 24 h, Figs. 4 d, e, S6 d, e).

Nighttime respiration per μ g Chl a initially increased on day 4, then decreased to nearly zero in both the HC and AC mesocosms on day 8 and remained relatively stable till the end of experiment. The elevated pCO₂ had a negative effect on phytoplankton respiration before day 12, but increased it thereafter, though no significant difference was observed between the HC and AC treatments (p = 0.834, Figs. 4 f, S6 f).

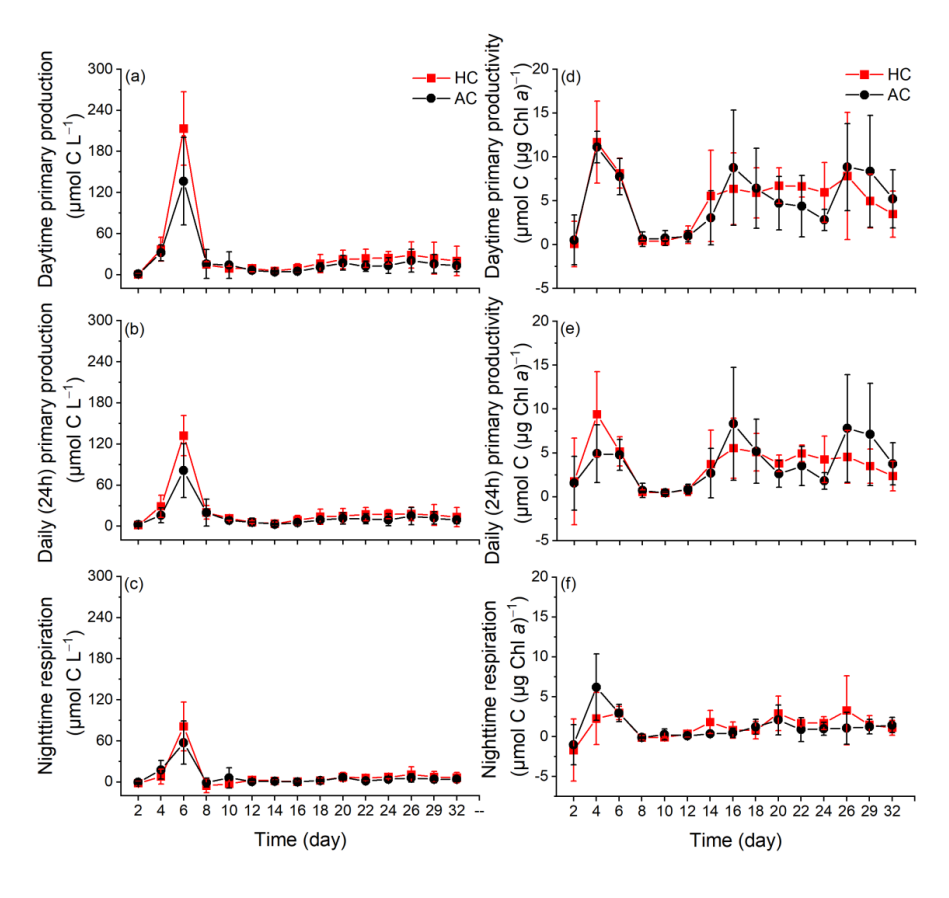


Figure 4. The changes of daytime primary production (a) and primary productivity (b), daily (24h) primary production (c) and primary productivity (d), nighttime respiration per water volume (e) and per Chl α (f) in HC (1000 μ atm) and AC (410 μ atm) mesocosms. Data are means \pm SD of 5 replicates for HC and 4 replicates for AC mesocosms.

300





273 3.4 Changes in Phytoplankton community and diversity A total of 47 genera identified microscopically include 33 genera of diatoms, 7 of 274 275 dinoflagellates, 2 of cyanobacteria, 2 of chlorophyta, 2 of cryptophyta and 1 of euglenophyta. In all 276 mesocosms, the dominant species included Cerataulina pelagica, Eucampia cornuta, Guinardia 277 delicatula, Leptocylindrus danicus, Skeletonema costatum, Protoperidinium sp., Gyrodinium spirale, Cryptophyta sp. and Pyramimonas sp. (Fig. S4). 278 279 Phytoplankton communities underwent dynamic succession in the mesocosms (Fig. 5). 280 Diatoms (mainly Cerataulina pelagica) dominated the phytoplankton communities during the early and middle stages of the experiment, as indicated by the similar temporal trends in total 281 phytoplankton and diatom cell counts compared with Chl a concentration (Figs. 5 a, b, S4 a). Diatom 282 283 density was lower in the HC than in the AC mesocosms, though the difference was not statistically significant (p = 0.259, Fig. S7 a). Autotrophic dinoflagellates began to emerge on day 8 and rapidly 284 285 declined on day 12 in both HC and AC enclosures (Fig. 5 c). Except for days 6 to 18, the elevated 286 pCO₂ increased the biomass of autotrophic dinoflagellates, though the difference was insignificant 287 (p = 0.505, Fig. S7 b). Hetero-dinoflagellates began to emerge on day 6, with their abundance 288 peaked on day 12 in the AC and on day 14 in the HC mesocosms, then decreased by day 22. The 289 elevated pCO_2 did not result in any significant change in terms of their cell numbers (p = 0.785, 290 Figs. 5 d, S7 c). On day 26, the biomass of hetero-dinoflagellates increased again in the HC 291 treatment, while it remained constant in the AC treatment (p = 0.729, Independent-samples t-test). 292 The biomass of small taxa (Cyanobacteria, Chlorophyta, Cryptophyta and Euglenophyta) 293 started to increase on day 8, the HC treatment significantly increased the total biomass of these 294 small phytoplankton species thereafter (p = 0.019, Figs. 5 e, S4 h, i, S7 d). From day 22, when 295 diatoms biomass decreased to the lowest level, the temporal variation in small taxa biomass became the main factor controlling overall phytoplankton dynamics (Figs. 5 e, S4 h, i). Accordingly, the 296 297 positive effect of HC on the small phytoplankton species led to an earlier transition of phytoplankton 298 from the large diatoms and dinoflagellate (mainly fall within the micro size fraction) to the smaller 299 ones (Fig. 6 a, b). This accelerated transition in the HC treatment was also evidenced by higher

concentration of POC and PON in the <20 µm fraction and lower concentration in the >20 µm





fraction (Figs. S2, S3).

In both HC and AC mesocosms, Shannon diversity index decreased sharply from day 2, reaching the lowest values on day 8 in AC mesocosms and on day 10 in HC mesocosms (Fig. S8 a). Before day 22, Shannon diversity index increased under elevated pCO_2 , whereas it is lowered under elevated pCO_2 level since day 24, although the differences were not statistically significant (p = 0.161, Fig. S8 b).

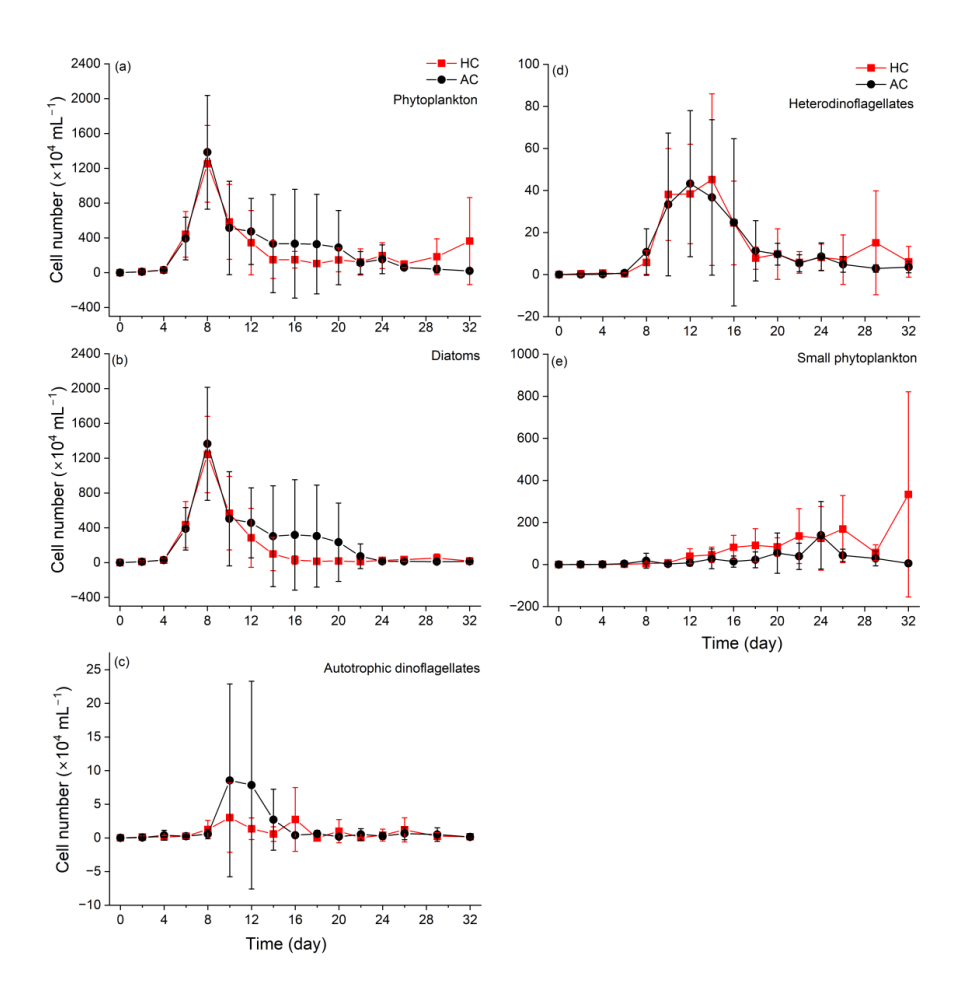


Figure 5. Temporal variations of phytoplankton (a), diatoms (b), photodinoflagellates (c), heterodinoflagellates (d) and (e) small phytoplankton (Cyanobacteria, Chlorophyta, Cryptophyta and Euglenophyta) cell numbers in HC (1000 μ atm) and AC (410 μ atm) mesocosms. Data are means \pm SD of 5 replicates for HC and 4 replicates for AC mesocosms.

315

316



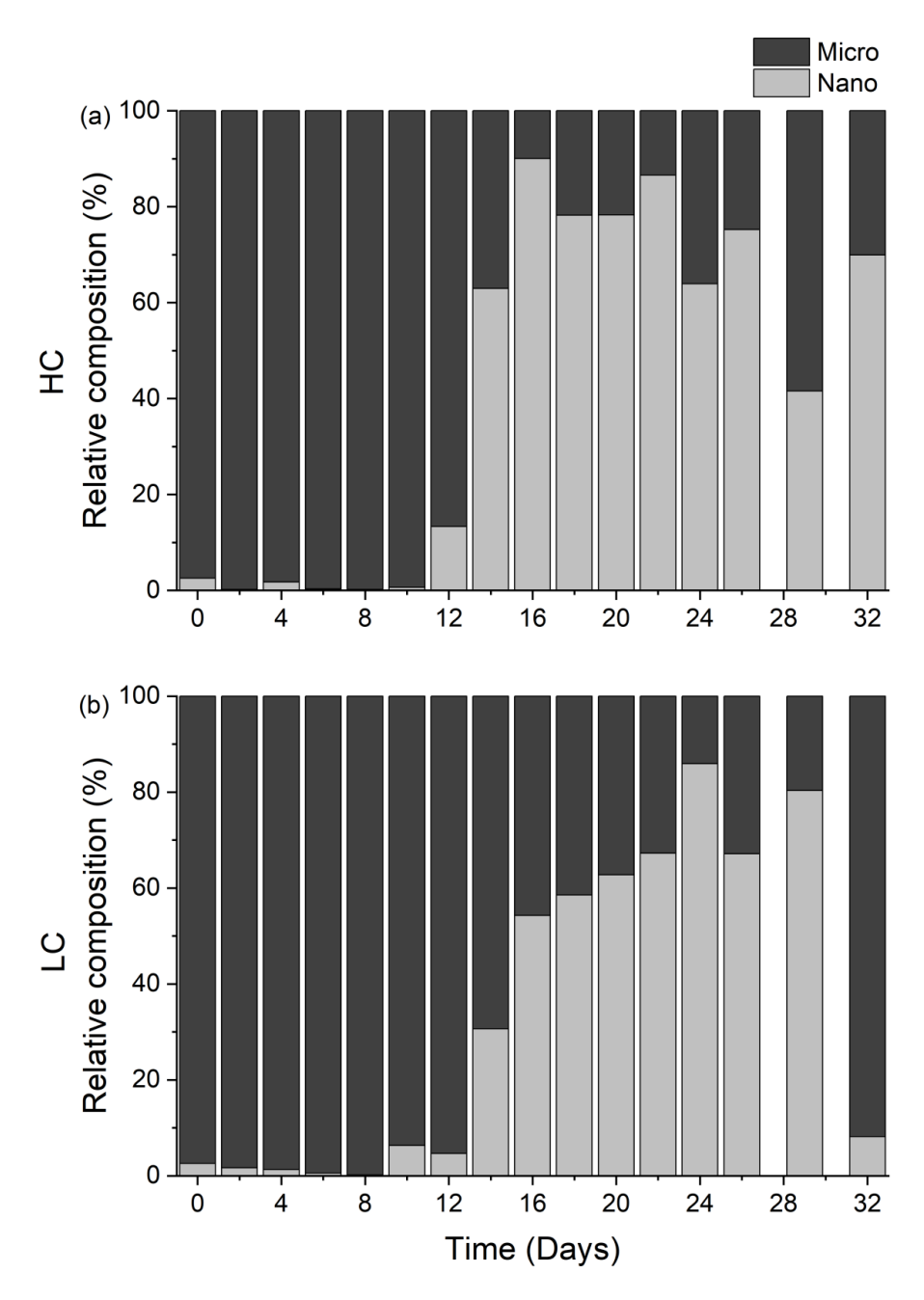


Figure 6. Temporal variations of the relative composition of diatoms + dinoflagellates (Diat + Dino, black), Cyanobacteria + Chlorophyta + Cryptophytes + Euglenophyta (Cyano + Chlo + Cryp + Eugl, grey) in HC (1000 μatm, a) and AC (410 μatm, b) mesocosms. Data are means of 5 replicates for





HC and 4 replicates for AC mesocosms.

318

317

319320

321

322

323

324

325

326327

328

329

330

331

332

333

334

335

336

337

338

339

340

341342

343

344

345

4 Discussion

diversity of phytoplankton due to physicochemical environmental changes (Henson et al., 2021; Yuan et al., 2020). Specifically, there appears a growing trend of increasing dinoflagellates abundance relative to diatoms (Carreto et al., 2018). Our mesocosm experiment, conducted in the highly eutrophic Wuyuan Bay in the southern East China Sea during late autumn, also indicated that elevated pCO₂, along with the natural decrease of surface water temperature and declined nutrient availability, altered the structure and diversity of phytoplankton community. The diatom dominance corresponded to the decreased diversity and evenness of phytoplankton community, while the diversity and evenness were recovered when the diatom dominance was replaced by dinoflagellates, however, this shift was relatively suppressed under elevated pCO₂ conditions. In our mesocosms, the dinoflagellates that emerged during the mid-phase (e.g., Protoperidinium sp., Pentapharsodinium dalei and Heterocapsa sp. Fig. S9 a) were predominantly small (<20 µm, Fig. S4 g) (Gu et al., 2013; Hanifah et al., 2022). Subsequently, these dinoflagellates were soon replaced by an even smaller size fraction, including Cyanobacteria, Chlorophyta, Cryptophytes, and Euglenophyta (Figs. 5, 6, S4). Ultimately, these smaller taxa maintained the primary production of phytoplankton communities after nutrient depletion (Fig. 4). When diatoms dominated the phytoplankton community (before day 8), elevated pCO2 had an insignificant negative effect on their biomass (Figs. 5 b, S7 a), but increased the primary production per water volume and per µg Chl a (Fig. 4 a, b, d and e). These may be attributed to the competitive advantages conferred by CO2-concentrating mechanisms (CCMs) in diatoms: their higher CO2 affinity and CCMs plasticity may help diatoms gain a competitive advantage in DIC uptake under ocean acidification scenarios (Huang et al., 2021; Raven and Beardall, 2020). Furthermore, the down-regulated of CCMs in diatoms can save energy for other physiology processes and thereby fuel their primary production (see the review by Gao and Campbell, 2014 and the references therein). These benefits resulting from elevated pCO₂ level also led to higher diversity and evenness (Fig. S8 a, b), suggesting that more diatom species were benefited from the elevated pCO₂, though the total

Ocean global changes have been suggested to alter community structure and reduce the

347

348349

350

351

352

353

354

355 356

357

358

359

360

361

362

363

364

365

366367

368

369

370371

372

373

374





demonstrated a positive effect of elevated pCO_2 on the photosynthetic carbon fixation by diatoms grown under low light and phytoplankton assemblages in waters of higher nutrient availability (Gao et al., 2022), our results (Figs. 5 b, S1) indicate that nutrient limitation can override or even reverse to the positive effects of elevated pCO_2 on diatoms (Boyd et al., 2016; Li et al., 2018). It appeared that dinoflagellates were less sensitive to the depletion of nutrients compared to diatoms, with autotrophic dinoflagellates were more sensitive to elevated pCO₂ (Figs. 5 c, S7 b). These suppressed transition from diatoms to autotrophic dinoflagellates under the elevated pCO₂ was consistent with our previous works (Huang et al., 2021), which is likely due to the different CCMs efficiency and/or acidic resilience between dinoflagellates and diatoms. Since the affinity of ribulose 1, 5-diphosphate carboxylase/oxidase (Rubisco) for CO₂ is much lower in autotrophic dinoflagellates than in diatoms (Reinfelder, 2011), elevated pCO₂ must have benefitted the former more compared the latter, though invisible growth advantage was observed on the autotrophic dinoflagellates between days 8 and 16. The heterodinoflagellates can utilize organic matters (Glibert and Legrand, 2006) and prey on microbes including bacteria and smaller microalgae (Jeong et al., 2010). This versatile nutrition strategy supported their rapid bloom starting from day 8, leading to the replacement of autotrophic ones from day 12 onward (Fig. 5 c, d). Although they were shown to be insensitive to ocean acidification (Meunier et al., 2017), their respiration was depressed due to the acidic stress, raising their resilience in terms of energetic cost (Wang and Gao, 2024). These mechanisms explain the observed insignificant effects of HC on hetero-dinoflagellates. The increases in NO₃⁻+NO₂⁻, PO₄³⁻ and SiO₃²⁻ concentrations from day 10 onward (Fig. 2 a, e, f) should be attributed to remineralization by heterotrophic bacteria (Arístegui et al., 2009; Bunse and Pinhassi, 2017). The gradual increase in SiO₃²⁻ concentration, a nutrient exclusively required by diatoms, coincided with their decline, confirming the low abundance of diatoms in the mid and late phase of experiment. These regenerated NO₃⁻+NO₂⁻ and PO₄³⁻ subsequently refueled the growth of small phytoplankton taxa, recover the diversity and evenness in the phytoplankton communities (Figs. 5 e, S8 a, b) (Thingstad and Rassoulzadegan, 1995). Alternatively, it is plausible that grazing activity by zooplankton, which was not quantifited in this study, also contributed to the apparent rise in diversity and evenness, as grazers tend to consume dominant phytoplankton taxa

diatom biomass was lower in HC mesocosms (Figs. S4, S7 a). While previous works have





375 (Thingstad and Rassoulzadegan, 1999; Calbet and Landry, 2004). 376 The dominant small taxa, such as *Cryptophyta* sp. and green microalga *Pyramimonas* sp. (Fig. 377 S4 h, i) during days 16–24, achieved primary productivity (per μg Chl a) comparable to the diatom-378 dominated community observed on days 4-6 (Fig. 4 b, d). The success of these small taxa can be 379 attributed to their small size and larger surface-to-volume ratio (Finkel et al., 2009; Giordano et al., 380 2005), which might enable them with higher efficiency in nutrients uptake and CO₂ diffusion. 381 Furthermore, the higher abundance of viruses and heterotrophic bacteria in the HC mesocosms 382 (Huang et al., 2021; Lin et al., 2018) intensified nutrient remineralization, subsidizing these small, 383 fast-growing phototrophs and leading to their earlier emergence on day 16 compared to day 24 in the AC mesocosms (Fig. 6). While it's possible that picophytoplankton originally present in this 384 region (Zhong et al., 2020) were missed by microscope-based identification in our mesocosm 385 386 experiment, it is reasonable to infer that they also contributed to the late-phase phytoplankton 387 communities. Previous studies indicated that, after diatom/dinoflagella blooms and nutrient 388 depletion, remineralized nutrients in the seawater may also favor the growth of picophytoplankton 389 (Nishibe et al., 2015; Fu et al., 2009) and elevated pCO₂ would further benefit their growth. Thus, 390 it is likely that, picophytoplankton also dominated the phytoplankton communities in the HC 391 mesocosms. 392 Previous studies have suggested that the shift from diatom to dinoflagellate dominance was 393 generally associated with declines in primary productivity (Huang et al., 2021; Cloern, 1996). The 394 results from the present autumn experiment reveals the same pattern with the previous spring 395 mesocosm experiment (Huang et al., 2021), indicating that it is not the seasonal temperature 396 trajectories but the availability of nutrients that controlled the shift. Such consistency underscores 397 that nutrient availability and stoichiometry are the primary determinants of phytoplankton 398 community composition, usually exerting stronger and more immediate effects on taxonomic and functional group dominance (Karl et al., 1996; Paerl and Paul, 2012; Ptacnik et al., 2008; Meyer et 399 400 al., 2016), though thermal and acidic stresses can impact photosynthesis and respiration to greater 401 extent under nutrient limitation (Li et al., 2018; Gao et al., 2022). 402 Reduced nutrient availability usually decreases phytoplankton community richness (Gazeau et

al., 2017), although ocean acidification appeared to partly offset such effects (Fig. S8). However,





404 these compensatory effects diminished once both the initial and regenerated nitrogen sources were 405 exhausted (after day 24, Fig. S8 b). At that point, only a few small phytoplankton taxa tolerant to low pH remained dominant, indicating a loss of diversity in the community and less stable 406 407 ecosystems (Mccann, 2000) under combination of acidic stress and nutrient limitation. Beyond 408 compensating previous works, our study further demonstrated that progressive ocean acidification is likely to reduce primary productivity and phytoplankton diversity in the eutrophicated coastal 409 410 water of the southern East China Sea. 411 **Data availability Statement** 412 All relevant data are presented in the papr and its Supporting Information file, and will be available upon request to the corresponding author Kunshan Gao. 413 **Conflict of Interest** 414 415 The authors declare no competing interests. 416 Acknowledgements 417 This study was supported by the National Key Research and Development Program of China (2022YFC3105303), the National Natural Science Foundation of China (42361144840, 418 419 41720104005). We are grateful to the engineers, Xianglan Zeng and Wenyan Zhao, for their 420 technical supports, and we thank Prof. Jian Ma (College of the Environment and Ecology, Xiamen 421 University) for providing the Environmental Water Analyzer (iSEA) during the mesocosm 422 experiment. 423 **Author's Contributions** 424 Kunshan Gao, Guang Gao and Xin Lin designed the mesocosm experiment; Yuming Rao, Na Wang, 425 Jiazhen Sun, Xiaowen Jiang, Di Zhang, Liming Qu, He Li, Qianqian Fu, Xuyang Wang, Cong Zhou, 426 Zichao Deng, Yang Tian, Xiangqi Yi, Ruiping Huang performed the mesocosm experiment; Yuming 427 Rao analyzed the data and wrote the manuscript; Na Wang performed microscopy observation; 428 Kunshan Gao edited the manuscript; All authors reviewed and contributed to revision of the 429 manuscript. 430 431 References 432 Arístegui, J., Gasol, J. M., Duarte, C. M., and Herndld, G. J.: Microbial oceanography of the dark ocean's





- 433 pelagic realm, Limnol. Oceanogr., 54, 1501-1529, https://doi.org/10.4319/lo.2009.54.5.1501, 2009.
- 434 Bach, L. T., Hernández-Hernández, N., Taucher, J., Spisla, C., Sforna, C., Riebesell, U., and Arístegui,
- 435 J.: Effects of Elevated CO₂ on a Natural Diatom Community in the Subtropical NE Atlantic, Front. Mar.
- 436 Sci, Volume 6 2019, 10.3389/fmars.2019.00075, 2019.
- 437 Bach, L. T., Taucher, J., Boxhammer, T., Ludwig, A., The Kristineberg, K. C., Achterberg, E. P., Algueró-
- 438 Muñiz, M., Anderson, L. G., Bellworthy, J., Büdenbender, J., Czerny, J., Ericson, Y., Esposito, M.,
- 439 Fischer, M., Haunost, M., Hellemann, D., Horn, H. G., Hornick, T., Meyer, J., Sswat, M., Zark, M., and
- 440 Riebesell, U.: Influence of Ocean Acidification on a Natural Winter-to-Summer Plankton Succession:
- 441 First Insights from a Long-Term Mesocosm Study Draw Attention to Periods of Low Nutrient
- 442 Concentrations, Plos One, 11, e0159068, 10.1371/journal.pone.0159068, 2016.
- 443 Boyd, P. W., Dillingham, P. W., McGraw, C. M., Armstrong, E. A., Cornwall, C. E., Feng, Y. y., Hurd, C.
- 444 L., Gault-Ringold, M., Roleda, M. Y., Timmins-Schiffman, E., and Nunn, B. L.: Physiological responses
- of a Southern Ocean diatom to complex future ocean conditions, Nat. Clim. Change., 6, 207-213,
- 446 10.1038/nclimate2811, 2016.
- 447 Bunse, C. and Pinhassi, J.: Marine Bacterioplankton Seasonal Succession Dynamics, Trends. Microbiol.,
- 448 25, 494-505, https://doi.org/10.1016/j.tim.2016.12.013, 2017.
- 449 Cai, W.-J., Hu, X., Huang, W.-J., Murrell, M. C., Lehrter, J. C., Lohrenz, S. E., Chou, W.-C., Zhai, W.,
- 450 Hollibaugh, J. T., and Wang, Y.: Acidification of subsurface coastal waters enhanced by eutrophication,
- 451 Nat. Geosci., 4, 766-770, 2011.
- 452 Calbet, A. and Landry, M. R.: Phytoplankton growth, microzooplankton grazing, and carbon cycling in
- 453 marine systems, Limnol. Oceanogr., 49, 51-57, https://doi.org/10.4319/lo.2004.49.1.0051, 2004.
- 454 Canadell, J. G., Monteiro, P. M., Costa, M. H., Cotrim da Cunha, L., Cox, P. M., Eliseev, A. V., Henson,
- 455 S., Ishii, M., Jaccard, S., and Koven, C.: Intergovernmental Panel on Climate Change (IPCC). Global
- 456 carbon and other biogeochemical cycles and feedbacks, in: Climate change 2021: The physical science
- 457 basis. Contribution of working group I to the sixth assessment report of the intergovernmental panel on
- dimate change, Cambridge University Press, 673-816, 2023.
- 459 Carreto, J. I., Carignan, M. O., Montoya, N. G., Cozzolino, E., and Akselman, R.: Mycosporine-like
- 460 amino acids and xanthophyll-cycle pigments favour a massive spring bloom development of the
- 461 dinoflagellate Prorocentrum minimum in Grande Bay (Argentina), an ozone hole affected area, J. Marine.





- 462 Syst., 178, 15-28, https://doi.org/10.1016/j.jmarsys.2017.10.004, 2018.
- 463 Chauhan, N., Dedman, C. J., Baldreki, C., Dowle, A. A., Larson, T. R., and Rickaby, R. E. M.: Contrasting
- 464 species-specific stress response to environmental pH determines the fate of coccolithophores in future
- des oceans, Mar. Pollut. Bull., 209, 117136, https://doi.org/10.1016/j.marpolbul.2024.117136, 2024.
- 466 Cloern, J. E.: Phytoplankton bloom dynamics in coastal ecosystems: A review with some general lessons
- 467 from sustained investigation of San Francisco Bay, California, Rev. Geophys., 34, 127-168,
- 468 https://doi.org/10.1029/96RG00986, 1996.
- 469 Engel, A., Zondervan, I., Aerts, K., Beaufort, L., Benthien, A., Chou, L., Delille, B., Gattuso, J.-P., Harlay,
- 470 J., and Heemann, C.: Testing the direct effect of CO₂ concentration on a bloom of the coccolithophorid
- 471 Emiliania huxleyi in mesocosm experiments, Limnol. Oceanogr., 50, 493-507, 2005.
- 472 Feng, Y., Xiong, Y., Hall-Spencer, J. M., Liu, K., Beardall, J., Gao, K., Ge, J., Xu, J., and Gao, G.: Shift
- 473 in algal blooms from micro- to macroalgae around China with increasing eutrophication and climate
- 474 change, Global Change Biol., 30, e17018, https://doi.org/10.1111/gcb.17018, 2024.
- 475 Finkel, Z. V., Beardall, J., Flynn, K. J., Quigg, A., Rees, T. A. V., and Raven, J. A.: Phytoplankton in a
- 476 changing world: cell size and elemental stoichiometry, J. Plankton. Res., 32, 119-137,
- 477 10.1093/plankt/fbp098, 2009.
- 478 Friedlingstein, P., O'Sullivan, M., Jones, M. W., Andrew, R. M., Hauck, J., Landschützer, P., Le Quéré,
- 479 C., Li, H., Luijkx, I. T., Olsen, A., Peters, G. P., Peters, W., Pongratz, J., Schwingshackl, C., Sitch, S.,
- 480 Canadell, J. G., Ciais, P., Jackson, R. B., Alin, S. R., Arneth, A., Arora, V., Bates, N. R., Becker, M.,
- 481 Bellouin, N., Berghoff, C. F., Bittig, H. C., Bopp, L., Cadule, P., Campbell, K., Chamberlain, M. A.,
- 482 Chandra, N., Chevallier, F., Chini, L. P., Colligan, T., Decayeux, J., Djeutchouang, L. M., Dou, X., Duran
- 483 Rojas, C., Enyo, K., Evans, W., Fay, A. R., Feely, R. A., Ford, D. J., Foster, A., Gasser, T., Gehlen, M.,
- 484 Gkritzalis, T., Grassi, G., Gregor, L., Gruber, N., Gürses, Ö., Harris, I., Hefner, M., Heinke, J., Hurtt, G.
- 485 C., Iida, Y., Ilyina, T., Jacobson, A. R., Jain, A. K., Jarníková, T., Jersild, A., Jiang, F., Jin, Z., Kato, E.,
- 486 Keeling, R. F., Klein Goldewijk, K., Knauer, J., Korsbakken, J. I., Lan, X., Lauvset, S. K., Lefèvre, N.,
- Liu, Z., Liu, J., Ma, L., Maksyutov, S., Marland, G., Mayot, N., McGuire, P. C., Metzl, N., Monacci, N.
- 488 M., Morgan, E. J., Nakaoka, S. I., Neill, C., Niwa, Y., Nützel, T., Olivier, L., Ono, T., Palmer, P. I., Pierrot,
- 489 D., Qin, Z., Resplandy, L., Roobaert, A., Rosan, T. M., Rödenbeck, C., Schwinger, J., Smallman, T. L.,
- 490 Smith, S. M., Sospedra-Alfonso, R., Steinhoff, T., Sun, Q., Sutton, A. J., Séférian, R., Takao, S., Tatebe,





- 491 H., Tian, H., Tilbrook, B., Torres, O., Tourigny, E., Tsujino, H., Tubiello, F., van der Werf, G.,
- 492 Wanninkhof, R., Wang, X., Yang, D., Yang, X., Yu, Z., Yuan, W., Yue, X., Zaehle, S., Zeng, N., and Zeng,
- 493 J.: Global Carbon Budget 2024, Earth Syst. Sci. Data, 17, 965-1039, 10.5194/essd-17-965-2025, 2025.
- 494 Fu, M., Wang, Z., Li, Y., Li, R., Sun, P., Wei, X., Lin, X., and Guo, J.: Phytoplankton biomass size
- 495 structure and its regulation in the Southern Yellow Sea (China): Seasonal variability, Cont. Shelf. Res.,
- 496 29, 2178-2194, https://doi.org/10.1016/j.csr.2009.08.010, 2009.
- 497 Gao, K.: Approaches and involved principles to control pH/pCO₂ stability in algal cultures, J. Appl.
- 498 Phycol, 33, 3497-3505, 2021.
- 499 Gao, K. and Campbell, D. A.: Photophysiological responses of marine diatoms to elevated CO₂ and
- decreased pH: a review, Funct. Plant. Biol., 41, 449-459, https://doi.org/10.1071/FP13247, 2014.
- 501 Gao, K., Zhao, W., and Beardall, J.: Future responses of marine primary producers to environmental
- 502 changes, Blue Planet, Red and Green Photosynthesis: Productivity and Carbon Cycling in Aquatic
- 503 Ecosystems, 273-304, 2022.
- 504 Gao, K., Gao, G., Wang, Y., and Dupont, S.: Impacts of ocean acidification under multiple stressors on
- 505 typical organisms and ecological processes, Mar. Life. Sci. Tech., 2, 279-291, 2020.
- Gao, K., Xu, J., Gao, G., Li, Y., Hutchins, D. A., Huang, B., Wang, L., Zheng, Y., Jin, P., and Cai, X.:
- 507 Rising CO₂ and increased light exposure synergistically reduce marine primary productivity, Nat. Clim.
- 508 Change., 2, 519-523, 2012.
- 509 Gattuso, J.-P., Magnan, A., Billé, R., Cheung, W. W., Howes, E. L., Joos, F., Allemand, D., Bopp, L.,
- 510 Cooley, S. R., and Eakin, C. M.: Contrasting futures for ocean and society from different anthropogenic
- 511 CO₂ emissions scenarios, Science, 349, aac4722, 2015.
- 512 Gazeau, F., Sallon, A., Pitta, P., Tsiola, A., Maugendre, L., Giani, M., Celussi, M., Pedrotti, M. L., Marro,
- 513 S., and Guieu, C.: Limited impact of ocean acidification on phytoplankton community structure and
- 514 carbon export in an oligotrophic environment: Results from two short-term mesocosm studies in the
- 515 Mediterranean Sea, Estuar. Coast. Shelf. S., 186, 72-88, https://doi.org/10.1016/j.ecss.2016.11.016, 2017.
- 516 Giordano, M., Norici, A., and Hell, R.: Sulfur and phytoplankton: acquisition, metabolism and impact on
- 517 the environment, New. Phytol., 166, 371-382, 2005.
- 518 Glibert, P. M. and Legrand, C.: The Diverse Nutrient Strategies of Harmful Algae: Focus on Osmotrophy,
- 519 in: Ecology of Harmful Algae, edited by: Granéli, E., and Turner, J. T., Springer Berlin Heidelberg, Berlin,





- 520 Heidelberg, 163-175, 10.1007/978-3-540-32210-8_13, 2006.
- 521 Gu, H., Luo, Z., Zeng, N., Lan, B., and Lan, D.: First record of Pentapharsodinium (Peridiniales,
- 522 Dinophyceae) in the China Sea, with description of Pentapharsodinium dalei var. aciculiferum,
- 523 Phycological Research, 61, 256-267, https://doi.org/10.1111/pre.12024, 2013.
- 524 Hanifah, A. H., Teng, S. T., Law, I. K., Abdullah, N., Chiba, S. U. A., Lum, W. M., Tillmann, U., Lim, P.
- 525 T., and Leaw, C. P.: Six marine thecate Heterocapsa (Dinophyceae) from Malaysia, including the
- 526 description of three novel species and their cytotoxicity potential, Harmful. algae., 120, 102338,
- 527 https://doi.org/10.1016/j.hal.2022.102338, 2022.
- 528 Hasle, G. R. and Syvertsen, E. E.: Chapter 2 Marine Diatoms, in: Identifying Marine Phytoplankton,
- 529 edited by: Tomas, C. R., Academic Press, San Diego, 5-385, https://doi.org/10.1016/B978-012693018-
- 530 4/50004-5, 1997.
- 531 Henson, S. A., Cael, B. B., Allen, S. R., and Dutkiewicz, S.: Future phytoplankton diversity in a changing
- 532 climate, Nat. Commun., 12, 5372, 10.1038/s41467-021-25699-w, 2021.
- 533 Huang, R., Sun, J., Yang, Y., Jiang, X., Wang, Z., Song, X., Wang, T., Zhang, D., Li, H., and Yi, X.:
- 534 Elevated pCO₂ Impedes Succession of Phytoplankton Community From Diatoms to Dinoflagellates
- Along With Increased Abundance of Viruses and Bacteria, Front. Mar. Sci, 8, 642208, 2021.
- 536 Jeong, H. J., Yoo, Y. D., Kim, J. S., Seong, K. A., Kang, N. S., and Kim, T. H.: Growth, feeding and
- 537 ecological roles of the mixotrophic and heterotrophic dinoflagellates in marine planktonic food webs,
- 538 Ocean. Sci. J., 45, 65-91, 10.1007/s12601-010-0007-2, 2010.
- 539 Karl, D. M., Christian, J. R., Dore, J. E., Hebel, D. V., Letelier, R. M., Tupas, L. M., and Winn, C. D.:
- Seasonal and interannual variability in primary production and particle flux at Station ALOHA, Deep-
- 541 Sea. Res. Pt. II, 43, 539-568, https://doi.org/10.1016/0967-0645(96)00002-1, 1996.
- 542 Li, F., Beardall, J., and Gao, K.: Diatom performance in a future ocean: interactions between nitrogen
- 543 limitation, temperature, and CO₂-induced seawater acidification, ICES. J. Mar. Sci., 75, 1451-1464,
- 544 10.1093/icesjms/fsx239, 2018.
- Li, Q., Wang, F., Wang, Z. A., Yuan, D., Dai, M., Chen, J., Dai, J., and Hoering, K. A.: Automated
- 546 Spectrophotometric Analyzer for Rapid Single-Point Titration of Seawater Total Alkalinity, Environ. Sci.
- 547 Technol., 47, 11139-11146, 10.1021/es402421a, 2013.
- 548 Lin, X., Huang, R., Li, Y., Li, F., Wu, Y., Hutchins, D. A., Dai, M., and Gao, K.: Interactive network





- 549 configuration maintains bacterioplankton community structure under elevated CO₂ in a eutrophic coastal
- 550 mesocosm experiment, Biogeosciences, 15, 551-565, 10.5194/bg-15-551-2018, 2018.
- 551 Liu, N., Tong, S., Yi, X., Li, Y., Li, Z., Miao, H., Wang, T., Li, F., Yan, D., Huang, R., Wu, Y., Hutchins,
- 552 D. A., Beardall, J., Dai, M., and Gao, K.: Carbon assimilation and losses during an ocean acidification
- 553 mesocosm experiment, with special reference to algal blooms, Mar. Environ. Res., 129, 229-235,
- 554 https://doi.org/10.1016/j.marenvres.2017.05.003, 2017.
- 555 Ma, J., Li, P., Chen, Z., Lin, K., Chen, N., Jiang, Y., Chen, J., Huang, B., and Yuan, D.: Development of
- 556 an Integrated Syringe-Pump-Based Environmental-Water Analyzer (iSEA) and Application of It for
- 557 Fully Automated Real-Time Determination of Ammonium in Fresh Water, Anal. Chem., 90, 6431-6435,
- 558 10.1021/acs.analchem.8b01490, 2018.
- 559 McCann, K. S.: The diversity-stability debate, Nature, 405, 228-233, 10.1038/35012234, 2000.
- 560 Meakin, N. G. and Wyman, M.: Rapid shifts in picoeukaryote community structure in response to ocean
- acidification, ISME J., 5, 1397-1405, 10.1038/ismej.2011.18, 2011.
- 562 Meunier, C. L., Algueró-Muñiz, M., Horn, H. G., Lange, J. A. F., and Boersma, M.: Direct and indirect
- 563 effects of near-future CO₂ levels on zooplankton dynamics, Mar. Freshwater. Res., 68, 373-380,
- 564 https://doi.org/10.1071/MF15296, 2017.
- Meyer, J., Löscher, C. R., Neulinger, S. C., Reichel, A. F., Loginova, A., Borchard, C., Schmitz, R. A.,
- 566 Hauss, H., Kiko, R., and Riebesell, U.: Changing nutrient stoichiometry affects phytoplankton production,
- 567 DOP accumulation and dinitrogen fixation a mesocosm experiment in the eastern tropical North
- 568 Atlantic, Biogeosciences, 13, 781-794, 10.5194/bg-13-781-2016, 2016.
- 569 Nishibe, Y., Takahashi, K., Shiozaki, T., Kakehi, S., Saito, H., and Furuya, K.: Size-fractionated primary
- 570 production in the Kuroshio Extension and adjacent regions in spring, J. Oceanogr., 71, 27-40,
- 571 10.1007/s10872-014-0258-0, 2015.
- 572 Paerl, H. W. and Paul, V. J.: Climate change: Links to global expansion of harmful cyanobacteria, Water.
- 573 Res., 46, 1349-1363, https://doi.org/10.1016/j.watres.2011.08.002, 2012.
- Paul, A. J. and Bach, L. T.: Universal response pattern of phytoplankton growth rates to increasing CO₂,
- 575 New. Phytol., 228, 1710-1716, https://doi.org/10.1111/nph.16806, 2020.
- 576 Ptacnik, R., Solimini, A. G., Andersen, T., Tamminen, T., Brettum, P., Lepistö, L., Willén, E., and
- 577 Rekolainen, S.: Diversity predicts stability and resource use efficiency in natural phytoplankton





- 578 communities, Proc. Natl. Acad. Sci., 105, 5134-5138, doi:10.1073/pnas.0708328105, 2008.
- Raven, J. A. and Beardall, J.: Energizing the plasmalemma of marine photosynthetic organisms: the role
- of primary active transport, J. Mar. Biol. Assoc. Uk., 100, 333-346, 2020.
- 581 Reinfelder, J. R.: Carbon concentrating mechanisms in eukaryotic marine phytoplankton, Annu. Rev.
- 582 Mar. Sci, 3, 291-315, 2011.
- 583 Riebesell, U., Bach, L. T., Bellerby, R. G., Monsalve, J. R. B., Boxhammer, T., Czerny, J., Larsen, A.,
- 584 Ludwig, A., and Schulz, K. G.: Competitive fitness of a predominant pelagic calcifier impaired by ocean
- 585 acidification, Nat. Geosci., 10, 19-23, 2017.
- 586 Ritchie, R. J.: Consistent sets of spectrophotometric chlorophyll equations for acetone, methanol and
- 587 ethanol solvents, Photosynth. Res., 89, 27-41, 2006.
- 588 Rogelj, J., Shindell, D., Jiang, K., Fifita, S., Forster, P., Ginzburg, V., Handa, C., Kheshgi, H., Kobayashi,
- 589 S., Kriegler, E., Mundaca,, and L., S., R., and Vilariño, M. V: Mitigation Pathways Compatible with
- 590 1.5°C in the Context of Sustainable Development, in: Global Warming of 1.5°C: IPCC Special Report
- 591 on Impacts of Global Warming of 1.5°C above Pre-industrial Levels in Context of Strengthening
- 592 Response to Climate Change, Sustainable Development, and Efforts to Eradicate Poverty, edited by:
- 593 Intergovernmental Panel on Climate, C., Cambridge University Press, Cambridge, 93-174, DOI:
- 594 10.1017/9781009157940.004, 2022.
- 595 Rokitta, S. D., John, U., and Rost, B.: Ocean acidification affects redox-balance and ion-homeostasis in
- the life-cycle stages of *Emiliania huxleyi*, Plos One, 7, e52212, 2012.
- 597 Schulz, K. G., Bellerby, R. G. J., Brussaard, C. P. D., Büdenbender, J., Czerny, J., Engel, A., Fischer, M.,
- 598 Koch-Klavsen, S., Krug, S. A., Lischka, S., Ludwig, A., Meyerhöfer, M., Nondal, G., Silyakova, A.,
- 599 Stuhr, A., and Riebesell, U.: Temporal biomass dynamics of an Arctic plankton bloom in response to
- 600 increasing levels of atmospheric carbon dioxide, Biogeosciences, 10, 161-180, 10.5194/bg-10-161-2013,
- 601 2013.
- 602 Steidinger, K. A. and Jangen, K.: Chapter 3 Dinoflagellates, in: Identifying Marine Phytoplankton,
- 603 edited by: Tomas, C. R., Academic Press, San Diego, 387-584, https://doi.org/10.1016/B978-012693018-
- 604 4/50005-7, 1997.
- Stukel, M. R., Irving, J. P., Kelly, T. B., Ohman, M. D., Fender, C. K., and Yingling, N.: Carbon
- 606 sequestration by multiple biological pump pathways in a coastal upwelling biome, Nat. Commun., 14,





- 607 2024, 10.1038/s41467-023-37771-8, 2023.
- 608 Tanaka, T., Alliouane, S., Bellerby, R. G. B., Czerny, J., de Kluijver, A., Riebesell, U., Schulz, K. G.,
- 609 Silyakova, A., and Gattuso, J. P.: Effect of increased pCO₂ on the planktonic metabolic balance during a
- mesocosm experiment in an Arctic fjord, Biogeosciences, 10, 315-325, 10.5194/bg-10-315-2013, 2013.
- Taylor, A. R., Brownlee, C., and Wheeler, G.: Coccolithophore cell biology: chalking up progress, Annu.
- 612 Rev. Mar. Sci, 9, 283-310, 2017.
- 613 Thingstad, T. F. and Rassoulzadegan, F.: Nutrient limitations, microbial food webs and 'biological C-
- 614 pumps': suggested interactions in a P-limited Mediterranean, Mar. Ecol. Prog. Ser., 117, 299-306, 1995.
- 615 Thingstad, T. F. and Rassoulzadegan, F.: Conceptual models for the biogeochemical role of the photic
- 516 zone microbial food web, with particular reference to the Mediterranean Sea, Prog. Oceanogr., 44, 271-
- 617 286, https://doi.org/10.1016/S0079-6611(99)00029-4, 1999.
- 618 Vázquez, V., León, P., Gordillo, F. J. L., Jiménez, C., Concepción, I., Mackenzie, K., Bresnan, E., and
- 619 Segovia, M.: High-CO₂ Levels Rather than Acidification Restrict Emiliania huxleyi Growth and
- 620 Performance, Microb. Ecol., 86, 127-143, 10.1007/s00248-022-02035-3, 2023.
- 621 Wang, N. and Gao, K.: Ocean acidification and food availability impacts on the metabolism and grazing
- 622 in a cosmopolitan herbivorous protist Oxyrrhis marina, Front. Mar. Sci, Volume 11 2024,
- 623 10.3389/fmars.2024.1371296, 2024.
- 624 Wu, Y., Campbell, D. A., and Gao, K.: Short-term elevated CO₂ exposure stimulated photochemical
- 625 performance of a coastal marine diatom, Mar. Environ. Res., 125, 42-48,
- 626 https://doi.org/10.1016/j.marenvres.2016.12.001, 2017.
- 627 Yang, S. and Liu, X.: Characteristics of phytoplankton assemblages in the southern Yellow Sea, China,
- 628 Mar. Pollut. Bull., 135, 562-568, 2018.
- 629 Yuan, Z., Liu, D., Masqué, P., Zhao, M., Song, X., and Keesing, J. K.: Phytoplankton Responses to
- 630 Climate-Induced Warming and Interdecadal Oscillation in North-Western Australia, Paleoceanogr.
- 631 Paleocl., 35, e2019PA003712, https://doi.org/10.1029/2019PA003712, 2020.
- 632 Zhong, Y., Liu, X., Xiao, W., Laws, E. A., Chen, J., Wang, L., Liu, S., Zhang, F., and Huang, B.:
- 633 Phytoplankton community patterns in the Taiwan Strait match the characteristics of their realized niches,
- 634 Prog. Oceanogr., 186, 102366, 2020.